Marsh, D., Watts, A., Maschke, W., & Knowles, P. F. (1978) *Biochem. Biophys. Res. Commun. 81*, 397.
Mason, T. L., Poyton, R. O., Wharton, D. C., & Schatz, G. (1973) *J. Biol. Chem. 248*, 1346.
Owicki, J. C., Springgate, M. W., & McConnell, H. M. (1978) *Proc. Natl. Acad. Sci. U.S.A. 75*, 1616.
Robinson, N. C., & Capaldi, R. A. (1977) *Biochemistry 16*, 375.
Scandella, C. J., Devaux, P., & McConnell, H. M. (1972) *Proc. Natl. Acad. Sci. U.S.A. 69*, 2056.
Schreier, S., Polnaszek, C. F., & Smith, I. C. P. (1978) *Biochim. Biophys. Acta 515*, 375.
Seelig, A., & Seelig, J. (1978) *Hoppe-Seyler's Z. Physiol. Chem. 359*, 1747.
Smith, I. C. P., Schreier-Muccillo, S., & Marsh, D. (1976) in *Free Radicals in Biology* (Pryor, W. A., Ed.) Vol. 1, Academic Press, New York.
Smith, L. (1955) *Methods Biochem. Anal. 2*, 427–434.
Stoffel, W., Zierenberg, O., & Scheefers, H. (1977) *Hoppe-Seyler's Z. Physiol. Chem. 358*, 865.
Takeuchi, Y., Ohnishi, S.-I., Ishinaga, M., & Kito, M. (1978) *Biochim. Biophys. Acta 506*, 54.
Träuble, H., & Haynes, D. H. (1971) *J. Membr. Biol. 7*, 324.
Träuble, H., & Sackmann, E. (1972) *J. Am. Chem. Soc. 94*, 4499.
Vaz, W. L. C., Vogel, H., Jähnig, F., Austin, R. H., & Schoellmann, G. (1978) *FEBS Lett. 87*, 269.
Vik, S. B., & Capaldi, R. A. (1977) *Biochemistry 16*, 5755.
Virji, M., & Knowles, P. F. (1978) *Biochem. J. 169*, 343.
Warren, G. B., Toon, P. A., Birdsall, N. J. M., Lee, A. G., & Metcalfe, J. C. (1974a) *Biochemistry 13*, 5501.
Warren, G. B., Toon, P. A., Birdsall, N. J. M., Lee, A. G., & Metcalfe, J. C. (1974b) *Proc. Natl. Acad. Sci. U.S.A. 71*, 622.
Watts, A., Marsh, D., & Knowles, P. F. (1978) *Biochem. Biophys. Res. Commun. 81*, 403.
Watts, A., Volotovski, I. D., & Marsh, D. (1979) *Biochemistry* (in press).
Yonetani, T., & Ray, G. S. (1965) *J. Biol. Chem. 240*, 3392.
Yu, C., Yu, L., & King, T. E. (1975) *J. Biol. Chem. 250*, 1383.

Phosphorus-31 Nuclear Magnetic Resonance Studies of Wild-Type and Glycolytic Pathway Mutants of *Saccharomyces cerevisiae*†

Gil Navon,‡ Robert G. Shulman,* Tetsuo Yamane, T. Ross Eccleshall,* Keng-Bon Lam,§ Jerald J. Baronofsky, and Julius Marmur

ABSTRACT: High-resolution phosphorus-31 nuclear magnetic resonance (^{31}P NMR) spectra of wild-type and mutant strains of *Saccharomyces cerevisiae* were observed at a frequency of 145.7 MHz. Levels of various phosphorus metabolites were investigated upon addition of glucose under both aerobic and anaerobic conditions. Three mutant strains were isolated and their biochemical defects characterized: *pfk* lacked phosphofructokinase activity; *pgi* lacked phosphoglucose isomerase activity; and *cif* had no glucose catabolite repression of the fructose bisphosphatase activity. Each mutant strain was found to accumulate characteristic sugar phosphates when glucose was added to the cell suspension. In the case of the phosphofructokinase deficient mutant, the appearance of a pentose shunt metabolite was observed. ^{31}P NMR peak assignments were made by a pH titration of the acid extract of the cells. Separate signals for terminal, penultimate, and central phosphorus atoms in intracellular polyphosphates allowed the estimation of their average molecular weight. Signals for glycero(3)phosphocholine, glycero(3)phosphoserine, and glycero(3)phosphoethanolamine as well as three types of nucleotide diphosphate sugars could be observed. The intracellular pH in resting and anaerobic cells was in the range 6.5–6.8 and the level of adenosine 5′-triphosphate (ATP) low. Upon introduction of oxygen, the ATP level increased considerably and the intracellular pH reached a value of pH 7.2–7.3, irrespective of the external medium pH, indicating active proton transport in these cells. A new peak representing the inorganic phosphate of one of the cellular organelles, whose pH differed from the cytoplasmic pH, could be detected under appropriate conditions.

Previous studies have shown the usefulness of high-resolution ^{31}P NMR[1] in monitoring intracellular concentrations of phosphate metabolites in suspensions of whole cells from mammalian (Moon & Richards, 1973; Henderson et al., 1974; Navon et al., 1977a, 1978; Evans & Kaplan, 1977) and microbial (Salhany et al., 1975; Navon et al., 1977b; Ugurbil et al., 1978) origins.

On the basis of chemical shifts of inorganic phosphate and other phosphate metabolites, the intracellular pH can be determined (Moon & Richards, 1973; Salhany et al., 1975; Navon et al., 1977a,b). In a previous study on endogenous

† From Bell Laboratories, Murray Hill, New Jersey 07974 (G.N., R.G.S., and T.Y.), and the Department of Biochemistry, Albert Einstein College of Medicine, Bronx, New York 10461 (T.R.E., K-B.L., J.J.B., and J.M.). *Received February 28, 1979.* Partial support for T.R.E. was from 1T32 AG 00052-01. Support for J.J.B. was from 5T32 GM 07128. Partial support for J.M. was obtained from 2P50 GM 19100. The part of this work done at Einstein was partially supported by 5R01 CA 12410.

‡ Permanent address: Department of Chemistry, Tel Aviv University, Ramat Aviv, Tel Aviv, Israel.
§ Present address: Connaught Laboratories, Ltd., Willowdale, Ontario, Canada M2N 5T8.

[1] Abbreviations used: DHAP, 1,3-dihydroxyacetone phosphate; FBP, fructose 1,6-bis(phosphate); F6P, fructose 6-phosphate; GAP, glyceraldehyde 3-phosphate; GPC, glycero(3)phosphocholine; GPE, glycero(3)phosphoethanolamine; GPS, glycero(3)phosphoserine; G6P, glucose 6-phosphate; NADH, β-nicotinamide adenine dinucleotide (reduced form); NADPH, β-nicotinamide adenine dinucleotide phosphate (reduced form); NAD^+, β-nicotinamide adenine dinucleotide (oxidized form); NMR, nuclear magnetic resonance; PEP, phosphoenolpyruvate; 3PGA, 3-phosphoglycerate; 6PGA, 6-phosphogluconate; P_i, inorganic phosphate; UDPG, uridinediphosphoglucose; YP, 1% Difco yeast extract + 2% Difco peptone; YPD, YP + 2% glucose; YPF, YP + 2% fructose; YPFGal, YP + 2% fructose + 2% galactose; YPGE, YP + 3% glycerol + 2% ethanol. Enzyme Commission numbers: phosphoglucoisomerase, 5.3.1.9; phosphofructokinase, 2.7.1.11; and fructose bisphosphatase, 3.1.3.11.

0006-2960/79/0418-4487$01.00/0

Table I: *S. cerevisiae* Strains

strain	phenotype	genotype
K8	wild type	α *leu1 trp5 ura1*
168-4b	fructose negative	α *cif ura1*
455-7d	slow growth on hexoses	α *pfk pyk*
BG-9A	wild type	α *ade2 ino1-13 ino4-8*
F2	glucose negative	α *ade2 ino1-13 ino4-8 pgi*

yeast cells under anaerobic conditions (Salhany et al., 1975), a rich ^{31}P NMR spectrum was observed, dominated by inorganic and polyphosphate peaks. The intracellular pH (pH_{in}) was found to be around 6.3 with only slight dependence on the extracellular pH (pH_{ex}). Other studies on *Escherichia coli* (Navon et al., 1977b) and ascites tumor cells (Navon et al., 1977a) showed that information on the flux of metabolites through the glycolytic pathway and the bioenergetics of the cells could be obtained when the cells were aerated and supplemented with a carbon source. Therefore, with the recent availability of glycolytic mutant strains of the yeast *Saccharomyces cerevisiae*, it was believed that ^{31}P NMR might prove useful in studying the metabolic blocks by monitoring their effects on the levels of phosphorylated metabolic intermediates.

Materials and Methods

Strains. The haploid yeast strains of *S. cerevisiae* used in this paper are listed in Table I. Strains 168-4b and 455-7d, derived from the wild-type K8, will be referred to as the catabolite-insensitive fructose bisphosphatase (*cif*) and phosphofructokinase (*pfk*) mutants, respectively. Strain F2, derived from the wild-type BG-9A, is the phosphoglucose isomerase (*pgi*) mutant strain.

Media and Growth. Strains were grown on a medium containing 1% (w/v) Difco yeast extract and 2% (w/v) Difco peptone (YP medium) supplemented with a carbon source at the following concentrations: 2% (w/v) glucose (YPD), 2% (w/v) fructose (YPF), 2% (w/v) fructose plus 2% (w/v) galactose (YPFGal), and 3% (v/v) glycerol plus 2% (v/v) ethanol (YPGE). To determine growth rates, we incubated the cultures in 300-mL sidearm flasks at 30 °C in a shaking water bath. Growth was monitored by measuring the turbidity in a Klett–Summerson photoelectric colorimeter equipped with a 600-nM filter.

Genetic Methods. Mutagenesis of strain K8 and selection of mutant strains 168-4b and 455-7d were performed by using the methodology described previously (Lam & Marmur, 1977). The mutant strain F2 was obtained from strain BG-9A, using an inositol selection procedure (Henry et al., 1975) and selecting colonies which grew on YPF but not on YPD plates.

For tetrad analysis, asci were dissected by the method of Johnston & Mortimer (1959) and linkage relationships determined by conventional tetrad analysis (Perkins, 1949).

Enzyme Assays. Cell cultures (10–15 mL) were harvested in the logarithmic or late logarithmic phase of growth by centrifugation. The pellet was washed once with deionized water and suspended in 0.4 mL of 1.0 M potassium phosphate buffer, pH 7.0. Cell extracts were made by disrupting cells with glass beads (0.45–0.5-mm diameter) in a Braun homogenizer using the adaptor which allows the use of small culture tubes (Needleman & Tzagoloff, 1975). The supernatant, obtained by centrifugation of the cell homogenate at 12000*g* for 30 min was assayed for enzyme activities at 25 °C by spectrophotometric methods. The assay protocols used were those described by Maitra & Lobo (1971) except those for fructose bisphosphatase, which was assayed according to Latzko & Gibbs (1974), and aldolase, which was assayed according to Richards & Rutter (1961) as modified by D. Fraenkel (personal communication).

In order to determine the effects of glucose on maltose permease activity, we grew cultures to the midlogarithmic phase on YP medium containing 2% (w/v) maltose and then glucose was added to 2% (w/v). At various times, aliquots were withdrawn, the cells harvested by centrifugation, the pellets washed once with deionized water, and the resuspended cells assayed for maltose permease activity using [U-^{14}C]-maltose according to the protocol of Serrano (1977).

Determination of Intracellular Levels of Glycolytic Intermediates. Cultures were grown to the midlogarithmic phase on YPGE medium, and then glucose was added to 2% (w/v). Aliquots were withdrawn at various times, the cells washed once with water, and the tubes placed immediately in a mixture of ethanol and dry ice to freeze the cells. The intracellular levels of glycolytic intermediates in perchloric acid extracts were determined enzymatically (Bergmeyer, 1974). The extracts were prepared by freezing and thawing the cells 3 times in cold 5% perchloric acid and centrifuging to obtain a supernatant which was then neutralized with 2 M K_2CO_3.

Preparation of Cells for NMR Spectroscopy. The wild-type strain K8, the *cif* and *pfk* mutants, in YPGE medium, and the *pgi* mutant, in YPFGal medium, were grown to the midlogarithmic phase at 30 °C. The cultures were immersed in ice-cold water and allowed to cool to 5 °C while being continuously aerated. The cells were centrifuged at low speed at 4 °C and washed twice with a minimal medium lacking nitrogen and carbon sources. The cells were suspended in a small volume of minimal medium, and D_2O was added to 10% final concentration. Cell extracts for analysis by NMR spectroscopy were prepared by vigorously shaking the cell suspension with 30% perchloric acid (prechilled to −20 °C), freezing and thawing 3 times, pelleting the cellular debris by centrifugation, neutralizing the supernatant with 2 M $KHCO_3$, centrifuging, passing the supernatant through a column of Chelex-100 resin, and finally adding D_2O and EDTA at final concentrations of 10% (v/v) and 20 mM, respectively.

All NMR measurements were performed with a Bruker HX 360 spectrometer with 10-mm sample tubes operated at 145.7 MHz for ^{31}P observation. A pulse angle of 60° was used. The repetition rates were 0.34 s for whole cell spectra and 1.36 for the cell extract spectra. In all spectra, broad-band proton irradiation was applied. Sample temperatures were maintained at 8 °C.

Chemicals and Enzymes. Glycolytic intermediates, enzymes, and coenzymes were purchased from Sigma Chemical Co. or from Boehringer Mannheim Corp. [U-^{14}C]Maltose was purchased from Amersham/Searle Corp. Other chemicals were reagent grade.

Results

The properties of the yeast mutants used in this study have not been previously reported. Hence, a preliminary characterization will be presented before the NMR spectra of the strains are described.

Mutant Defective in Phosphofructokinase Activity. Mutant strain (*pfk*) 455-7d grows well on YPGE medium but poorly on YPD and YPF media (Table II), and in general its growth on media containing hexoses is impaired. In cell extracts assayed for glycolytic enzyme activities, the phosphofructokinase level was lower than in the wild-type strain when parent and mutant strains were grown on YPD or YPGE medium (Table III). It was later observed that the mutant also had essentially no detectable pyruvate kinase activity when the

Table II: Doubling Times of Yeast Strains Growing in YP Medium Containing Different Carbon Sources[a]

carbon source	strain K8	168-4b (*cif*)	455-7d (*pfk*)	BG-9A	F2 (*pgi*)
glucose	1.8	4.3[b]	6.0	1.8	no growth
fructose	2.8	no growth	5.5	2.8	4.5
glucose + fructose	1.5	2.9[c]	9.5[b]	1.8	no growth
galactose	2.5	3.2[c]	2.5[d,e]	4.5[d]	no growth
glycerol + ethanol	4.3	2.8	2.9	3.7	no growth
glucose + glycerol + ethanol	1.8	3.1	3.5	–[f]	–
glucose + glycerol	1.7	3.2[c]	5.0	–	–
glucose + ethanol	1.8	3.5[b]	4.5[e]	–	–
fructose + glycerol	1.8	no growth	–	–	–
fructose + ethanol	1.8	no growth	–	–	–
glycerol	4.1	3.5	3.9[e]	–	–
ethanol	5.2	4.5	3.7[d,e]	–	–
maltose	2.2	6.9	2.5	–	–
sucrose	2.3	2.2[c]	–	–	–

[a] Doubling times expressed in hours are for strains grown at 30 °C, with shaking, on YP medium containing glucose, fructose, galactose, maltose, or sucrose at a concentration of 2% (w/v), ethanol at a concentration of 2% (v/v), and/or glycerol at a concentration of 3% (v/v). [b] Growth occurs after a lag of ~12 h. [c] Growth occurs after a lag of 24 h. [d] Growth on this hexose (or disaccharide) is nonfermentative. [e] Growth is restricted to three or four generations. [f] A minus indicates not determined.

Table III: Specific Activities of Glycolytic Pathway Enzymes[a]

enzyme	strain K8	168-4b (*cif*)	455-7d (*pfk*)	BG-9A	F2 (*pgi*)
hexokinase (glucose as substrate)	0.16	0.35	0.26	0.32	0.64
hexokinase (fructose as substrate)	0.69	0.93	0.79	0.66	2.0
phosphoglucose isomerase	0.74	1.27	0.89	1.35	0.001
phosphofructokinase	0.17	0.32	0.005	0.34	0.75
fructose bisphosphatase	0.06	0.06	0.06	0	0
aldolase	0.37	0.15	0.16	0.19	0.36
triosephosphate isomerase	0.3	0.2	0.14	0.13	0.11
glyceraldehyde-3-phosphate dehydrogenase	3.52	4.30	3.29	4.54	8.96
phosphoglycerate kinase	1.48	1.29	1.31	1.81	4.18
phosphoglycerate mutase	0.99	0.95	0.85	0.72	0.84
enolase	0.48	0.79	0.39	0.66	0.65
pyruvate kinase	1.41	1.16	0.01	2.12	2.69

[a] Enzymes were assayed as indicated under Materials and Methods. Strains K8 and 168-4b (*cif*) were grown on YPGE medium, and strains BG-9A and F2 (*pgi*) were grown on YPFGal medium. The values given are in units per milligram of protein. One unit of activity = 1 μmol of β-nicotinamide adenine dinucleotide phosphate (oxidized or reduced)/min at 25 °C. Protein was determined by using the procedure of Lowry et al. (1951).

strain was grown on YPGE or YPD medium. Tetrad analysis of spores from two different crosses with wild-type haploid strains showed that the mutational lesions, giving rise to a lack of phosphofructokinase activity and a lack of pyruvate kinase activity, segregated as independent nuclear mutations, consistent with it being a double mutant. The explanation for the ability of this mutant to use hexoses as a carbon source is under investigation. It is interesting to note that the product of the phosphofructokinase reaction, FBP, is a positive effector of pyruvate kinase. A strain carrying only the *pfk* mutation

Table IV: Levels of Glycolytic Intermediates in Wild-Type and *cif* Mutant Strains[a]

	wild-type strain K8		*cif* mutant	
	A	B	A	B
glucose 6-phosphate	0.2	0.3	0.4	5.8
fructose 6-phosphate	0.05	0.1	0.2	1.3
fructose bis(phosphate)	2.5	9.3	2.6	51.5
dihydroxyacetone phosphate	0.5	1.9	0.4	3.9
3-phosphoglycerate	0.4	1.2	0.7	3.7
2-phosphoglycerate	0.04	0.1	0.07	0.3
phosphoenolpyruvate	0.1	0.1	0.1	0.5
ATP	1.00	2.1	1.00	0.4

[a] The values of the glycolytic intermediates expressed as micromoles per gram dry weight were determined as described under Materials and Methods. Column A shows the levels of intermediates for cells grown on YPGE medium. Column B shows the levels of intermediates for cells grown on YPGE medium 30 min after the addition of glucose to the medium.

appeared to have slightly more phosphofructokinase activity than the double mutant.

Mutant Defective in Phosphoglucose Isomerase Activity. The mutant strain F2 (*pgi*), which was selected for its ability to grow on YPF medium but not on YPD medium, can grow only in rich medium containing fructose, as shown in Table II. However, the addition of glucose, glucosamine, maltose, or sucrose inhibits growth even in the presence of fructose. This mutant strain is unable to grow on any defined medium tested so far. The analysis of tetrad data for spores obtained as the result of crossing this strain with a wild-type tester strain and sporulating the diploid strain shows that the mutation is at a single site and, as expected, inherited in a Mendelian fashion. The F2 strain is revertable on YPD at a frequency of 3×10^{-8} but is not revertable on YPGE medium.

When cell extracts were assayed for the activities of glycolytic enzymes and compared to the parent strain grown under similar conditions, the only difference was the virtual absence of phosphoglucose isomerase activity in the mutant strain (Table III). Thus, this mutant strain was designated as phosphoglucose isomerase negative (*pgi*).

Mutant with Altered Fructose 1,6-Bisphosphatase Properties. This mutant strain (*cif*) was selected for its ability to grow on YPGE medium but only poorly on YPD medium. It does not grow at all on YPF medium. The doubling times for growth on different carbon sources are shown in Table II. This strain will only begin to grow on a medium containing glucose after a lag of 12–24 h. This strain grows well on media containing nonfermentative carbon sources or galactose as the carbon source. Glucose does not inhibit growth on a medium containing glycerol plus ethanol as the carbon sources. When the glycolytic pathway enzymes were assayed for activity, no differences were observed in comparison to the parent strain. However, when glucose was added to cells grown on YPGE medium and cell extracts were assayed for fructose 1,6-bisphosphatase activity after various times of exposure to glucose, the activity of this enzyme did not progressively decrease as occurs in the wild-type strain K8 (Figure 1A). The mutation does not affect another glucose-repressible enzyme, maltose permease, which is repressed by glucose in the mutant strain (Figure 1B). Hence, the catabolite insensitivity of glucose-repressible enzymes is not a general effect of the mutation. Cells grown on YPGE medium to which glucose has been added build up a high level of glycolytic intermediates, especially FBP, as compared to the wild-type strain (Table IV). However, the level of ATP decreases in the mutant strain whereas it increases in wild-type cells (Table IV and data not

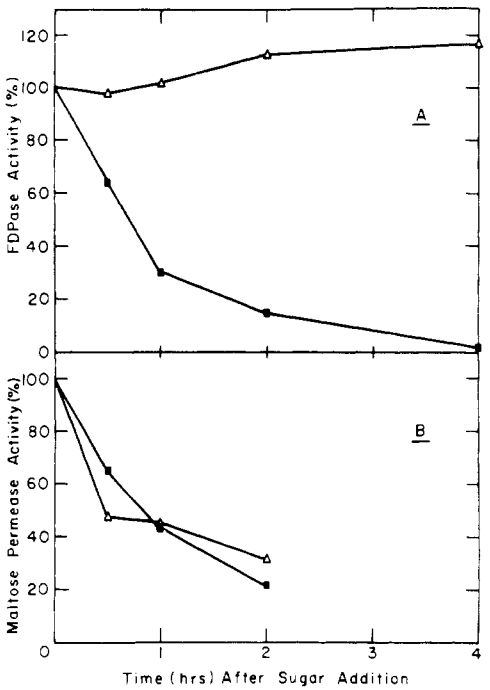

FIGURE 1: Levels of fructose 1,6-bisphosphatase (A) and maltose permease (B) activities in the wild-type and mutant strains after addition of glucose to the growth medium. The strains were grown to the midlogarithmic phase in YPGE medium (A) or YP medium containing 2% (w/v) maltose (B), and then glucose was added to 2% (w/v). Aliquots were withdrawn at various times and the enzyme activities determined as indicated under Materials and Methods. The initial specific activity of fructose 1,6-bisphosphatase was 8.7×10^{-2} and 10.0×10^{-2} μmol/(min mg of protein) for the wild-type strain K8 and the *cif* mutant strain, respectively. The initial maltose permease specific activity was 0.43 and 0.31 nmol/(min mg dry wt) in the wild-type strain K8 and the *cif* mutant strain, respectively. Enzyme activity from the wild-type strain (■); for the *cif* mutant (△) after glucose addition.

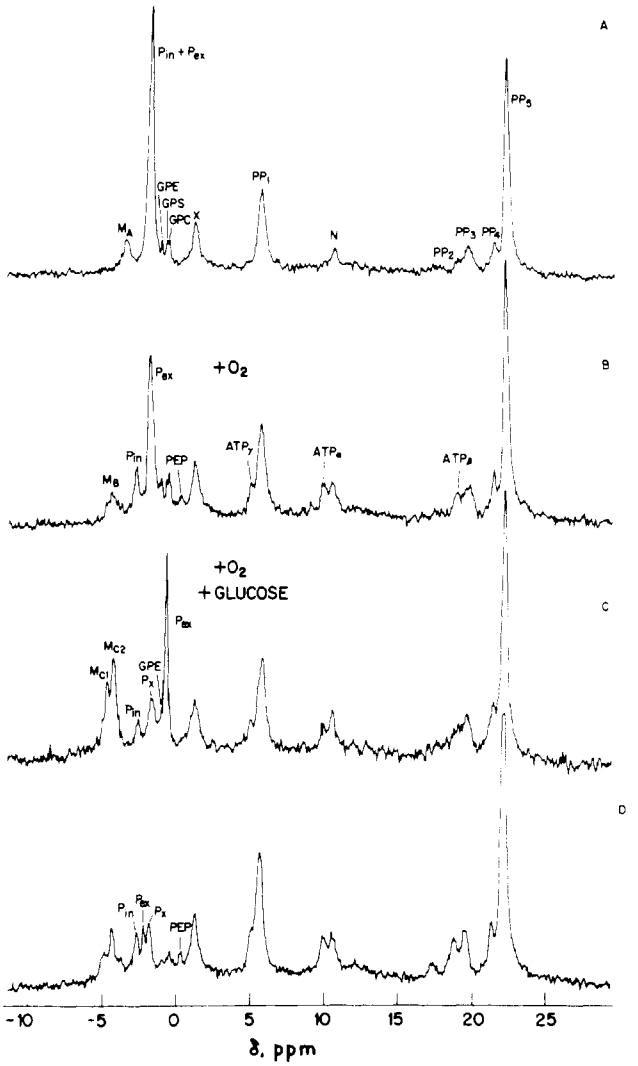

FIGURE 2: ^{31}P NMR spectra of wild-type yeast cells. Strain K8 was grown on YPGE medium. The cells were sedimented, washed twice with minimal medium, and resuspended in an equal volume of salt solution containing 7 mM phosphate buffer, pH 6.0. The spectra were taken ~3 h after harvesting. Cells were kept at 0 °C before measurement. All spectra were taken with either 1000 or 2000 scans of 60° pulses with a 0.34-s repetition rate. Glucose was added to a final concentration of 50 mM at 30 min. (A) Resting cells; at time zero, O_2 bubbling was started at a rate of 13 cm^3/min and continued throughout the experiment; (B) accumulations obtained between 13 and 23 min; (C) accumulations between 36 and 41 min; and (D) accumulations between 105 and 115 min.

shown). The addition of fructose instead of glucose also inhibits the growth of cells on YPGE medium and leads to the accumulation of hexose phosphates (data not shown). Thus, the inability to utilize fructose as a carbon source is not due to an inability to phosphorylate the fructose, which is confirmed in the hexokinase assay using fructose as substrate. Fructose 1,6-bisphosphatase activity is not inhibited by the presence of fructose, unlike the wild-type strain.

The recessive mutation that causes this phenotype was shown by tetrad analysis to be consistent with a nuclear mutation located at a single site. It has been located on chromosome II and linked to the *lys2* locus. This mutant is revertable at a frequency of 3×10^{-8}. Many properties of the *cif* mutant appear to be similar to those of a mutant obtained in *S. carlsbergensis* by van de Poll & Schamhart (1977).

NMR Spectra of Wild-Type Yeast. Figure 2 shows the 145.7-MHz ^{31}P NMR spectra of wild-type yeast cells before and after aeration and addition of glucose to the medium. Each spectrum was a sum of 1000 or 2000 free induction decays lasting 0.34 s for a total of 5 or 10 min. Figure 2A shows the spectrum of the cellular suspension immediately after resuspension in the NMR tube. This spectrum is quite similar to that published earlier (Salhany et al., 1975) of resting yeast cells. The peaks can be assigned from the previous work as well as from the extract spectrum presented here and by other comparisons discussed in this paper. Starting from low field (at the left), the resonances are assigned as follows. The resonance M_A is assigned to 3-phosphoglyceric acid (3PGA) on the basis of its position and from a previous report (Solomos, 1970). The next intense peak is due to inorganic phosphate. In other experiments under similar conditions (data not shown) and in experiments with mutant strains described subsequently, the signal of the inorganic phosphate was split into two peaks with roughly equal intensities representing intracellular phosphate (P_{in}) and external phosphate (P_{ex}). In this particular experiment $pH_{in} = pH_{ex}$, resulting in the superposition of the two peaks. They split, however, with a concomitant decrease in the intensity of P_{in} when oxygen is bubbled through the cell suspension (Figure 2B). The next three weak lines in Figure 2A are glycero(3)phosphoethanolamine (GPE), glycero(3)phosphoserine (GPS), and glycero(3)phosphocholine (GPC). Since the chemical shift of the GPC is pH independent, it was used as an internal standard and was added to the solution when necessary. Its chemical shift was measured as 0.49 ppm downfield from 85% H_3PO_4 contained in a capillary tube. The peak labeled X and occurring at +1 ppm has not been

identified. It is not pH dependent so that assignment to a phosphodiester bond is likely, particularly in view of its position which is close to the tRNA phosphate peak at +0.5 ppm. The next peak, PP_1, is the sum of several terminal phosphate resonances from phosphate sequences including $P_2O_7^{4-}$. Peak N is in the region containing both NAD^+ and NADH. However, from spectra of the perchloric acid extract shown in Figure 6 it is seen to be predominantly NAD^+. Peaks PP_2, PP_3, and PP_4 in Figure 2A are penultimate phosphates from polyphosphate chains, including the middle phosphate of tripolyphosphate $P_3O_{10}^{5-}$. Finally, PP_5 comes from the inner peaks of longer polyphosphates.

Figure 2B shows the spectrum after O_2 bubbling has started. Several significant changes are observed. First, the P_{in} peak has moved to lower field, indicating that pH_{in} is 7.3 while pH_{ex} is 6.5. Although this peak is shown as well separated from the P_{ex} peak, by taking spectra at intermediate times after the onset of respiration, it is possible to see P_{in} move away from the combined peak to lower fields. As a consequence of the high internal pH, it can be seen that the peak in the phosphomonoester region (M_B) has also moved to lower field and once again its position is in agreement with that expected for 3PGA at the measured value of internal pH. Continuing to higher field, the small peak at 0.34 ppm is assigned to PEP on the basis of its chemical shift. Finally, the three peaks labeled ATP_γ, ATP_α, and ATP_β are at the positions expected, under these conditions, for the three phosphates of ATP. However, in the intact cell spectrum it is not possible to distinguish among the peaks of the different nucleotide triphosphates. The levels of nucleotide triphosphates in yeast cells have been previously determined to be 4.8, 1.5, 1.5, and 1.1 nmol/mg dry wt for ATP, GTP, UTP, and CTP, respectively (Kudrna & Edlin, 1975). The levels of deoxyribonucleotide triphosphates are an order of magnitude lower. Thus, ATP is the predominant nucleotide triphosphate in the cell.

Figure 2C shows the effects of adding 50 mM glucose. Two peaks appear in the phosphomonoester region, and from the titration of the cell extracts seen in Figures 4 and 5 it is concluded that M_{C1} consists mainly of G6P while M_{C2} includes contributions from FBP and F6P as well as some other compounds which have similar chemical shifts and pH dependences. Immediately after glucose is added, peak M_{C1} is more intense than M_{C2}, while subsequently the relative intensities are reversed as can be seen in Figure 2C. From the chemical shifts of M_{C1} and M_{C2} it is possible to determine that pH_{in} is $\sim$7.0. This helps to identify the internal phosphate peak P_{in} since its chemical shift corresponds to P_i at pH 7.2, which agrees, within the accuracy of the method, with that of the sugar phosphates. Its intensity is reduced by approximately a factor of 2 upon the addition of glucose. The next peak, P_x in the inorganic phosphate region, reflects a pH of 6.5. Hence, it arises neither from the part of the cell (presumably the cytoplasm) containing the sugar phosphates nor from the external medium which has a pH of $\sim$3.6, corresponding to the next inorganic phosphate peak, P_{ex}. Since the mitochondrial pH should be higher than the cytoplasmic pH, as has been shown in liver cells by using ^{31}P NMR (Cohen et al., 1978), peak P_x probably does not come from mitochondrial inorganic phosphate. The most logical assignment of P_x is to the vacuoles storing polyphosphate.

Finally, Figure 2D shows the spectrum starting 75 min after glucose addition, presumably after the glucose has been depleted. The G6P peak is much weaker than before, and the position of the remaining phosphomonoester corresponds to either FBP or 3PGA. Three inorganic phosphate peaks are still observed with a considerable reduction in the P_{ex} peak, particularly by comparison with the starting spectrum. The intensity of the polyphosphate region has increased considerably, indicating the accumulation of inorganic phosphate in this form. The levels of ATP and PEP in this spectrum are similar to those observed for oxygenated yeast cells before the addition of glucose (Figure 2B).

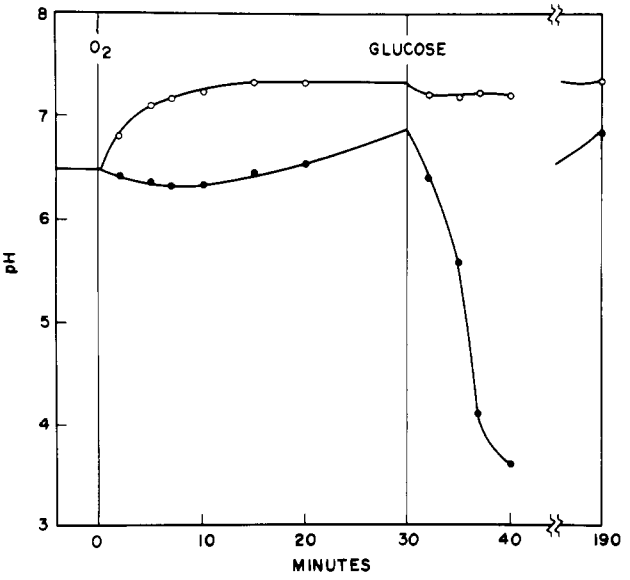

FIGURE 3: Internal and external pH values in aerobic wild-type yeast obtained from the NMR spectra in Figure 2. (○) Internal pH; (●) external pH.

The changes in intracellular and external pH values during the experiment as measured from the chemical shifts of the inorganic phosphate are given in Figure 3.

To help identify the peaks, we made a perchloric acid extract of cells, shortly after the addition of glucose, a stage corresponding to several minutes prior to spectrum 2C. Figure 4 shows the pH dependence of the low-field region of these spectra, while Figure 5 is a plot of the chemical shifts vs. pH. From these results it is possible to identify the α and β anomers of G6P as contributing most of the intensity of the largest peak at the low-field end of the spectrum, to identify the α anomer of FBP as the lowest field peak, and to assign two peaks to β-FBP and a nearby peak to F6P. Hence, with the exception of some intensity from weak unassigned peaks, the sugar phosphate region is assigned to glycolytic intermediates. The large peak in the center of the spectra shown in Figure 4 is inorganic phosphate. The chemical shifts of the three higher field resonances are identical with GPE, GPS, and GPC. It should be noted that in the plot of Figure 5 the former two peaks do show a slight pH dependence at the highest pH values (they fall above the horizontal line) since the serine and ethanolamine residues titrate in basic solutions.

Spectra of the extracts in the high-field regions are shown in Figure 6 for $6.0 < pH < 8.9$. Since these extracts have passed through a Chelex column and contain 10 mM EDTA, the divalent metal ion concentration is very low, in contrast to the intact cells, which results in differences between the two kinds of spectra. As shown in the well-resolved spectrum at pH 7.55 in Figure 6B, it is possible to identify terminal phosphate peaks from ATP_γ, ADP_β, $P_3O_{10}^{5-}$, and $P_2O_7^{4-}$ in the region between +4.5 and +8.0 ppm. All but the last are split by spin–spin couplings to the nonidentical penultimate phosphate groups. The lowest field group marked "END" consists of peaks which have been assigned to terminal

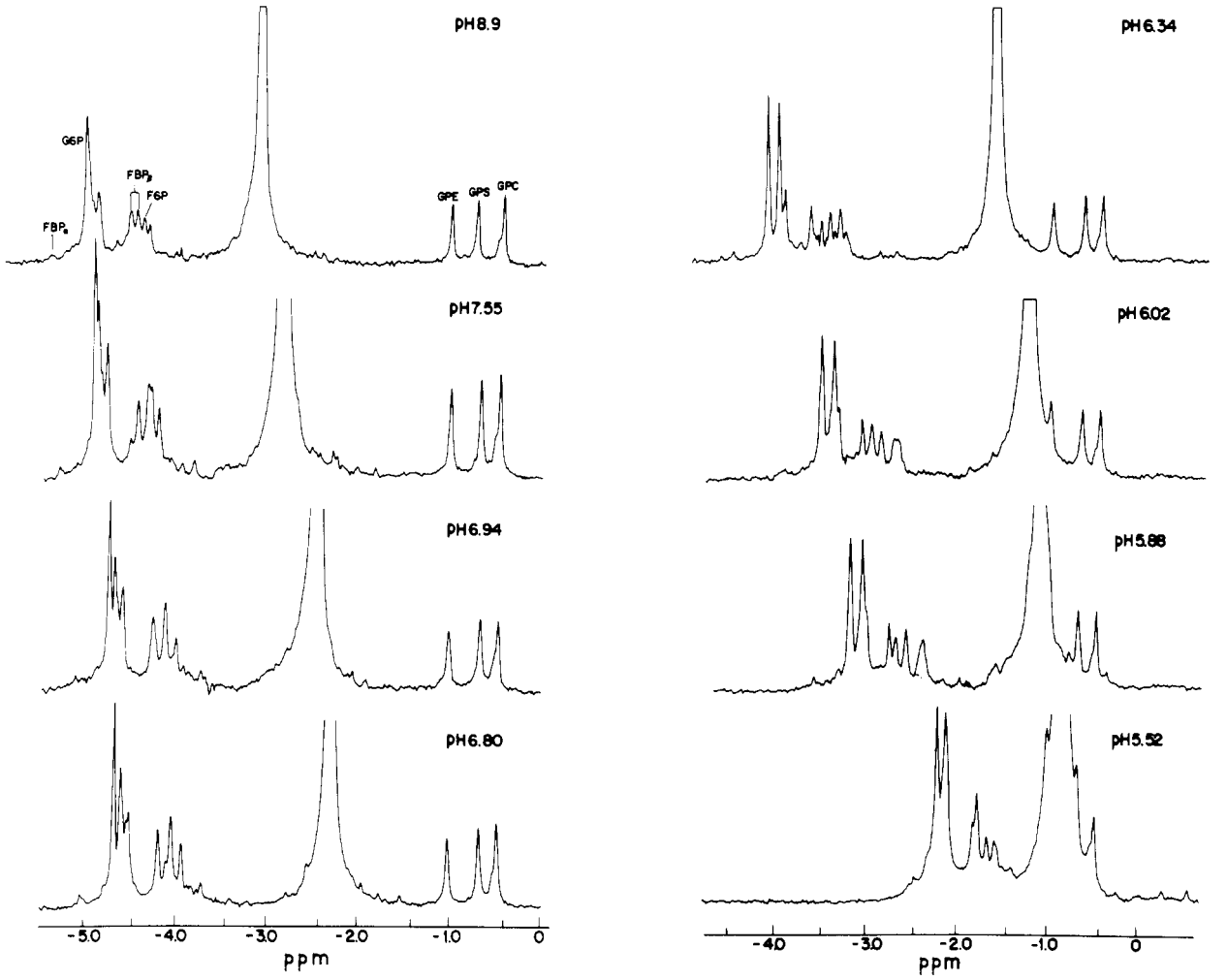

FIGURE 4: Titration of the perchloric acid extract spectrum of wild-type yeast under aerobic conditions showing the low-field region on an expanded scale. The extract was prepared 15 min after introduction of 50 mM glucose, during which time the cells were kept at 0 °C with O_2 bubbling. Preparation of the extracts is described under Materials and Methods.

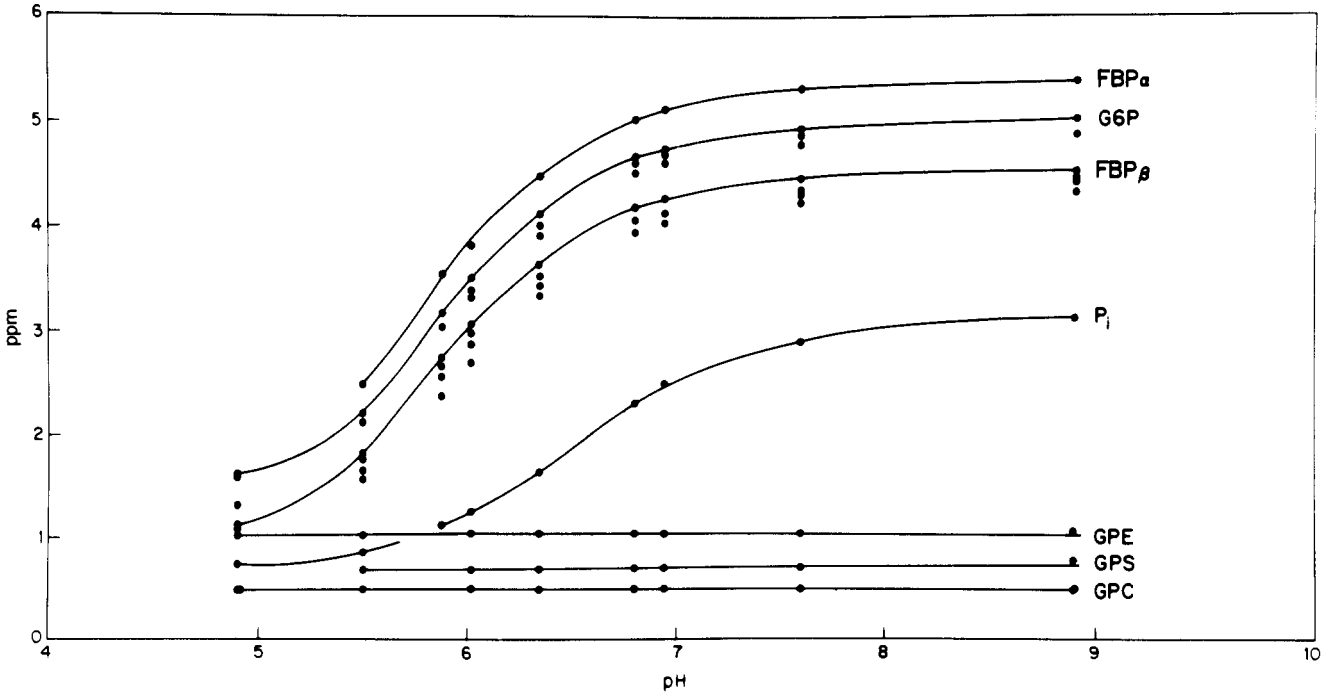

FIGURE 5: Titration plot of the positions of the peaks shown in Figure 4.

phosphates from chains longer than the tripolyphosphate. The broadening of the signal in this region may arise from small differences in the terminal phosphate positions. As the pH falls to 6.0, most of these peaks move to higher field and

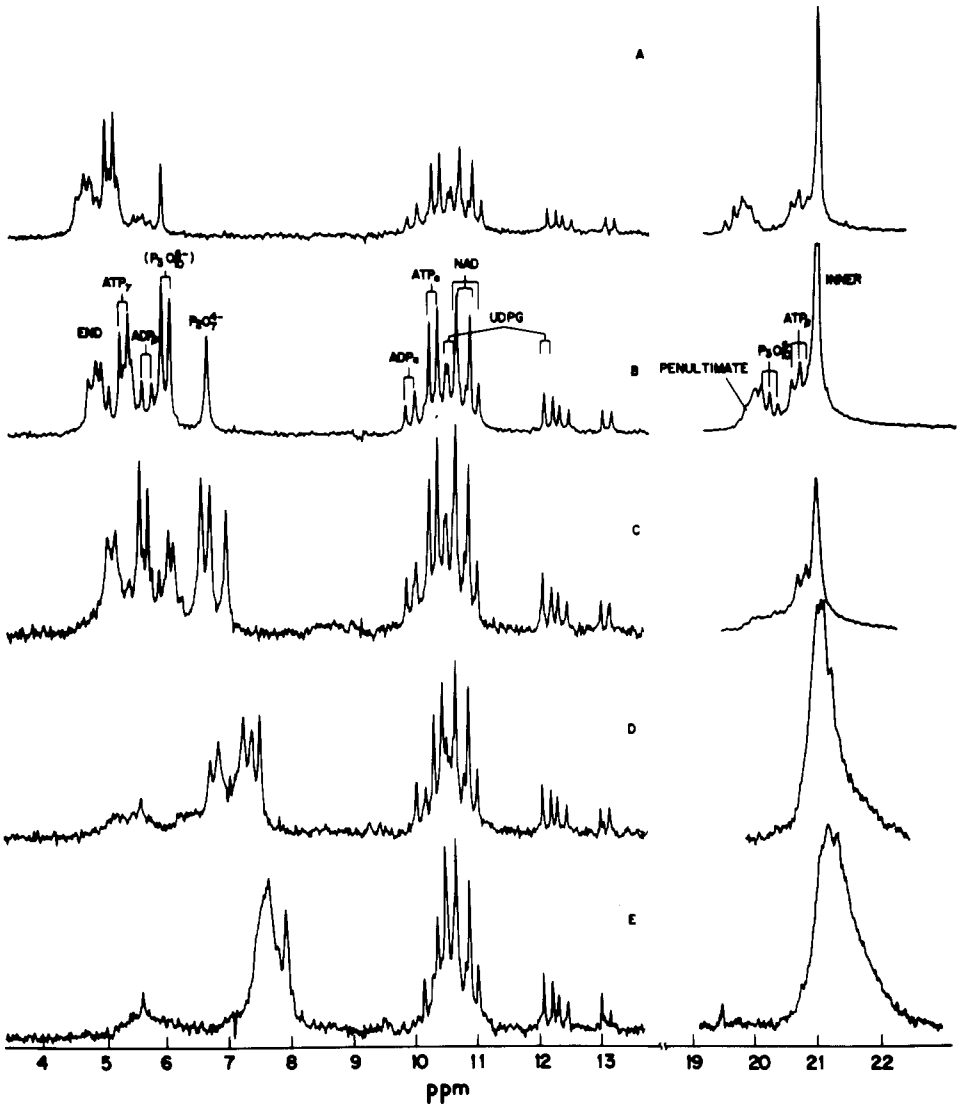

FIGURE 6: Perchloric acid extract spectra of wild-type yeast under aerobic conditions at high pH values. The sample was the same as that used for Figure 4. The high field region is shown. (A) pH 8.9; (B) pH 7.55; (C) pH 6.94; (D) pH 6.34; and (E) pH 6.02.

coalesce so that individual assignments are not possible, except for the $P_2O_7^{4-}$ singlet which remains resolved. The effect of divalent metal ions is to lower the pK of terminal phosphates. In the spectra of the intact cell (PP_1 in Figure 2), the terminal phosphate peak was broad enough to include these various resolved resonances and its chemical shift was ~5.7 ppm. It is clear that this position in conjunction with the weights of the different components can be used to determine the pH and free divalent metal ion concentration in the phosphate storage vacuoles.

NMR Spectra of the Glycolytic Mutant Strains. The ^{31}P NMR spectra of three different glycolytic mutants were investigated and compared with wild-type cells measured under similar conditions. Figure 7A shows the spectra of the *pfk* mutant measured after the cells were introduced into the NMR tube, under the same conditions as those used for wild-type cells in Figure 2A. Peak M_A, as mentioned above, is consistent with Solomos' determination of high 3PGA concentrations in starved cells (Solomos, 1970). There is a residual ΔpH as determined by the splitting of P_{in} and P_{ex} which corresponds to pH_{in} 6.7 and pH_{ex} 6.2 and a high concentration of internal inorganic phosphate as judged from the intensity of the P_{in} NMR peak. Further upfield a GPC peak can be seen, but neither GPE nor GPS is observed. Finally, in the +12-ppm region, peak U, which includes contributions from UDPG and similar compounds, is more intense in this mutant, while the polyphosphate peak PP_5 is weaker. After oxygenation starts, the ΔpH increases; pH_{in} becomes 7.3 while pH_{ex} becomes 6.1. The considerable reduction in intensity of the P_{in} peak is primarily explained by the appearance of ATP, whose peaks are labeled in Figure 7B. The ATP terminal phosphate (peak ATP_γ) is particularly well separated from the PP_1 peak, which is at a slightly higher field position than that seen in Figure 2B. Introducing glucose results in a rapid buildup of peak M_{C1}, which, as seen in the extract spectra of Figures 7E and 8B, has a large contribution from G6P, and of peak M_{C2}, with a large contribution from F6P. Figure 7C also shows a dramatic reduction in the intensities of the ATP resonances and of the P_{in} peak. This peak is so weak that once again it has been identified by calculating pH_{in} from the G6P position and noting that the chemical shift of P_i expected at this pH agrees with the position of the small peak labeled P_{in} in the figure. These observations are in perfect accord with the characterization of this mutant having a phosphofructokinase deficiency. Introducing glucose has depleted both P_{in} and ATP by phosphorylating the glucose. Furthermore, after P_i and ATP are depleted (Figure 7D), no further glucose is phosphorylated. Finally, a very interesting peak observed at the lowest field position in the extract spectrum (Figures 7E and 8B) has been identified as 6-phosphogluconic acid (6PGA), an intermediate

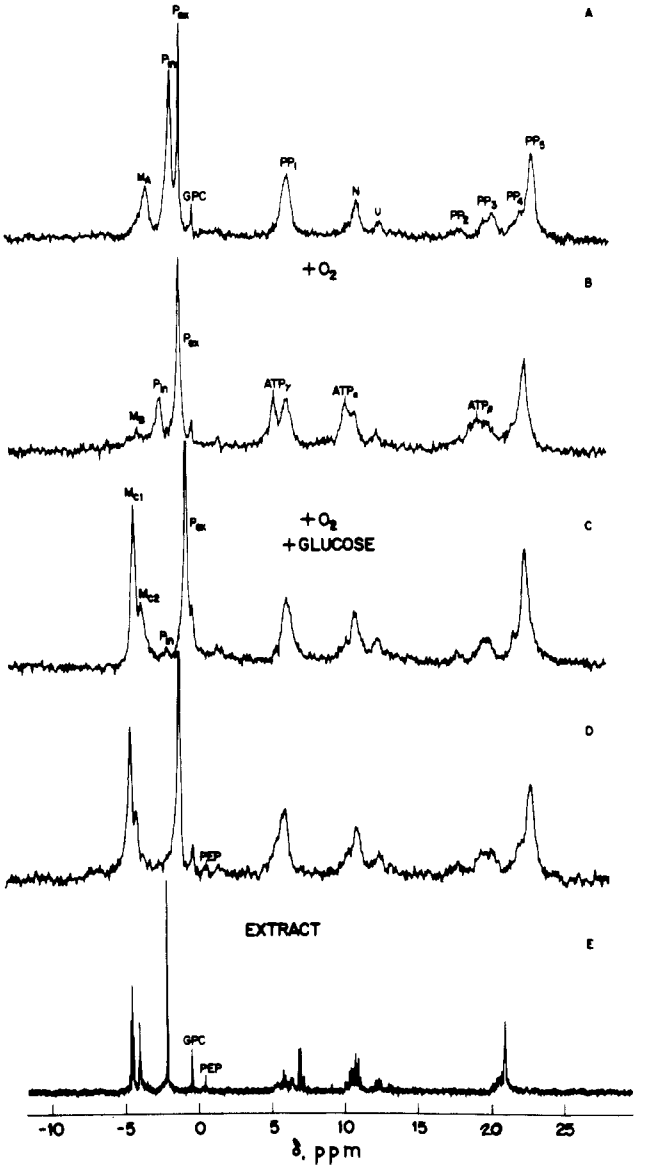

FIGURE 7: ^{31}P NMR spectra obtained for the *pfk* mutant. The conditions of growth of the strain and the preparation of the cells were the same as those used in Figure 2. For calibration of the chemical shifts, 0.5 mM GPC was added. 1000 60° pulses were accumulated for each whole-cell spectrum. At time zero, O_2 bubbling was started and continued until spectrum D was accumulated. After 40 min, glucose was added to a final concentration of 100 mM. (A) Resting cells; (B) accumulations obtained between 20 and 25 min; (C) 2000 scans accumulated between 41 and 51 min; (D) 1000 scans accumulated between 74 and 79 min; and (E) extract prepared immediately after spectrum D was accumulated, with pH adjusted to 6.86.

of the pentose shunt. This indicates that the *pfk* mutant has increased the flux through the pentose shunt trying to bypass the blocked phosphofructokinase. It is possible that the unassigned peaks in the sugar phosphate region such as the signal indicated by Z in Figure 8B may be other intermediates of the pentose shunt. Other interesting metabolic changes are the appearance of PEP in Figure 7D, which is also observed in the spectrum of the extract (Figure 7E), and the weak intensity of the signal at a position corresponding to signal X in Figure 2.

The effect of glucose addition to the *pfk* mutant under anaerobic conditions is shown in Figure 9. The same sugar phosphates are observed as in Figure 7C, but the relative concentration of G6P (M_{B1} in Figure 9B) is smaller under anaerobic conditions. As in the aerobic experiment, no ATP is observed following the addition of glucose. However, in contrast to observations in Figure 7, the P_{in} peak is not reduced. The chemical shifts of the inorganic phosphate peaks correspond to pH_{in} 6.8, pH_{ex} 6.3 and pH_{in} 6.6, pH_{ex} 6.2 before and after the addition of glucose, respectively.

In the spectra for the *cif* mutant shown in Figure 10A, all peaks are the same as those observed previously and indicate that pH_{in} is 6.7 and pH_{ex} is 6.1. The effects of O_2 bubbling shown in Figure 10B are that both P_{in} and P_{ex} shift to lower fields, indicating slightly higher pH values (pH_{in} 7.1, pH_{ex} 6.4), and ATP is formed. Introducing 100 mM glucose generates sugar phosphate peaks at the G6P position (peak M_{C1}) and the FBP region (peak M_{C2}) as seen in the Figure 10C. Furthermore, the P_{in} peak is reduced to such a level that it cannot be observed. A few minutes later, the sugar phosphate region has changed so that most of the signal intensity is in the FBP region (Figure 10D). This peak is indeed almost exclusively FBP as can be seen from the spectra of the cell extracts (Figures 8C and 10E). Figure 11 shows the effect of glucose added under anaerobic conditions. Once again the sugar phosphate peak is almost entirely composed of FBP, the P_{in} peak is slightly reduced by the glucose addition, and no ATP is formed. The pH values before and after glucose addition are pH_{in} 6.7, pH_{ex} 6.3 and pH_{in} 6.4, pH_{ex} 6.0, respectively.

The analysis of the last mutant, *pgi*, is particularly clear-cut since it lacks phosphoglucose isomerase activity so that glycolysis cannot proceed beyond G6P. The spectra for resting cells shown in Figure 12A are essentially similar to those of the previous cells except for the relatively small NAD^+ peak and a very intense peak for the polyphosphate inner groups. There are two peaks from inorganic phosphate to a ΔpH of 0.5 (pH_{in} 6.9, pH_{ex} 6.4). However, the addition of O_2 collapses the ΔpH and there is no buildup of ATP. It should be noted that, in contrast to the three previous yeast preparations which were grown on YPGE, the *pgi* mutant was grown on YPFGal medium. Thus, these cells are not capable of respiration because fructose represses mitochondrial function. Upon adding glucose, the G6P concentration slowly increases (seen in parts C and D of Figure 12) and the time course of this increase is shown in Figure 13. After more than 1 h of exposure to glucose, the perchloric acid extract shows only a G6P signal dominating the sugar phosphate region (see Figures 8D and 12E). Presumably the slow rate of glucose phosphorylation is determined by the depressed energy state of these cells, no ATP being observed in the extract. The spectrum of the extract at higher fields shows few signals, with no peaks being observed in the UDPG region. An interesting observation in Figure 12 is that aerated yeast cells can have a high level of polyphosphate with no evidence for the existence of any appreciable amount of ATP. The reduced polyphosphate peak in the extract is caused by the perchloric acid extraction, possibly due to the insolubility or hydrolysis of the polymer.

Discussion

The NMR spectra presented show how this approach can be exploited to study metabolic change in vivo. While many results were predictable from growth and biochemical studies, some, however, were not. In this section results concerning yeast cell metabolism in general will be discussed first, followed by those obtained for the three mutant strains.

From the NMR spectra it is possible to follow the intracellular pH in a straightforward manner. In most of the spectra, the inorganic phosphate peak was split into two components. The chemical shift of one of them agreed with

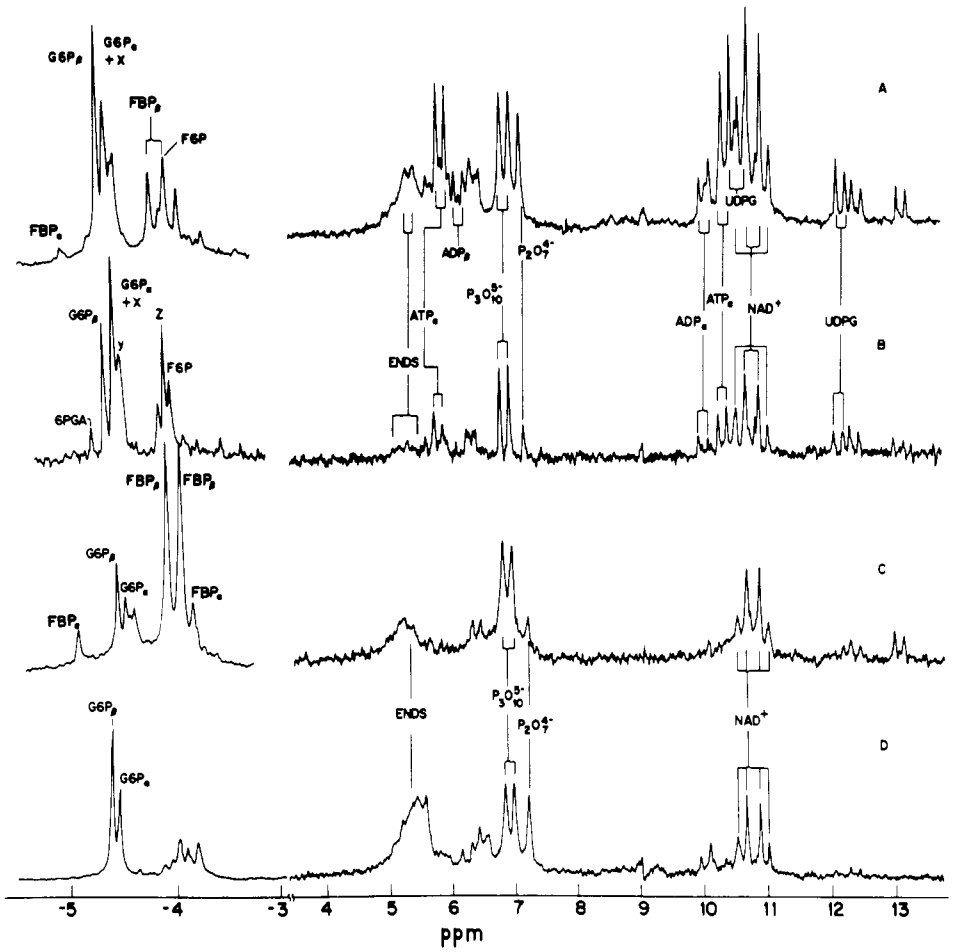

FIGURE 8: Comparison of extracts of wild-type and mutant strains incubated at 8 °C with glucose during O_2 bubbling. (A) K8 wild-type, pH 6.94; (B) *pfk* mutant, pH 6.86; (C) *cif* mutant, pH 6.76; and (D) *pgi* mutant, pH 6.86.

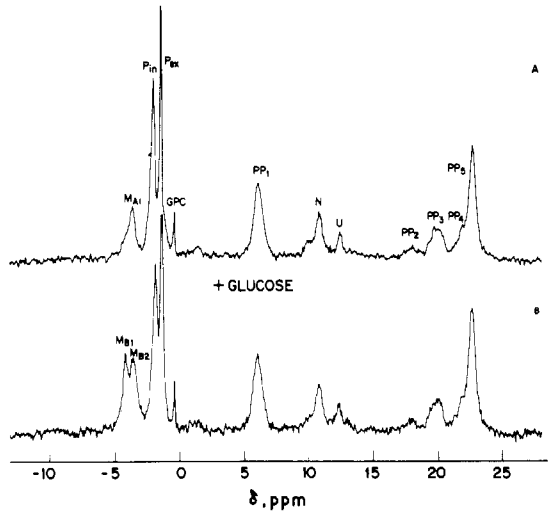

FIGURE 9: ^{31}P NMR spectra of the *pfk* mutant under anaerobic conditions. Each spectrum consists of 2000 accumulations. (A) Resting cells; (B) accumulations obtained between 12 and 22 min after addition of 100 mM glucose.

the pH of the external medium as measured with a pH meter. Thus, the other component was assigned to intracellular inorganic phosphate and its chemical shift used for the determination of the intracellular pH. In those spectra with a very weak intracellular P_i signal, the chemical shifts of the sugar phosphates could be used to determine the intracellular pH. This is illustrated in Figures 2C, 7C, and 10C, in which strong signals for G6P and FBP were obtained as a consequence of the addition of glucose to the cells. However, such a determination is less accurate than that based on the chemical shift of P_i, owing to some overlap with other sugar phosphates and a more pronounced dependence on Mg^{2+} concentration (Burt et al., 1976).

The chemical shift of P_i is not affected by Mg^{2+} ions. Also, any affect by paramagnetic metal ions on the chemical shift of P_i is absent since paramagnetic metal ions would significantly shift the positions of all compounds and this was not observed. It is concluded that the position of the intracellular P_i peak reflects the real intracellular pH.

A very interesting result is the observation of three peaks in the chemical shift region characteristic of inorganic phosphate (Figure 2C). One of the peaks (P_{ex}) was assigned to external phosphate since its position was that predicted from the pH meter reading. The second peak (P_{in}) was assumed to be the cytoplasmic P_i since its position agreed within 0.2 pH unit of that calculated from the chemical shifts of the sugar phosphates. The third peak, designated as P_x in Figure 2C, was thought to be the P_i inside one of the organelles with a pH corresponding to 6.5. It could not be assigned to the mitochondrion because respiring mitochondria would be expected to have a more alkaline pH, by Mitchell's hypothesis (Mitchell & Moyle, 1969; Rottenberg, 1975), than the cytoplasm. The most likely assignment of P_x is to the vacuoles which contain polyphosphates.

The detection of P_x illustrates one of the advantages of the NMR method over those based on the distribution of weak acids or weak bases (Rottenberg, 1975). In cells containing various organelles, these methods give an average pH of the

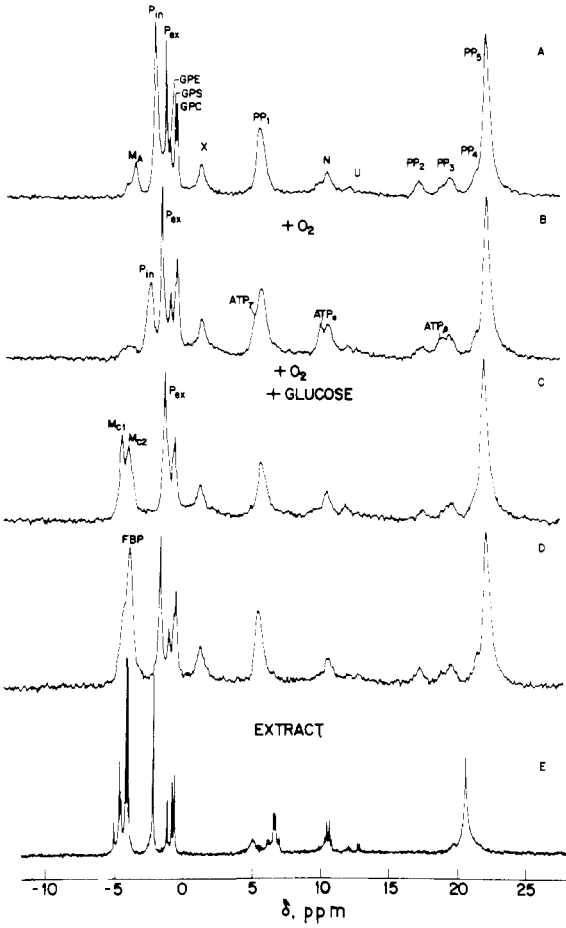

FIGURE 10: ^{31}P NMR spectra obtained for the *cif* mutant. The conditions of growth and the preparation of the cells were the same as those used in Figure 2. For calibration of the chemical shifts, 1 mM GPC was added. After 30 min, glucose was added to a final concentration of 100 mM. (A) Resting cells (2000 scans); at time zero, O_2 bubbling was started; (B) accumulations obtained between 4 and 14 min (2000 scans); (C) accumulations obtained between 33 and 38 min (1000 scans); (D) accumulations obtained between 110 and 115 min (1000 scans); and (E) extract prepared immediately after spectrum D was accumulated, with pH adjusted to 6.76.

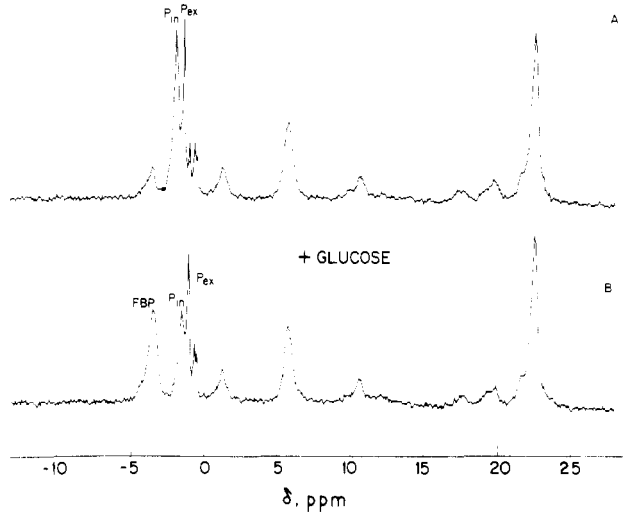

FIGURE 11: ^{31}P NMR spectra of the *cif* mutant under anaerobic conditions. (A) Resting cells; (B) accumulations obtained between 15 and 20 min after the addition of 100 mM glucose.

cytoplasmic and organelle pH reflecting the distribution of the probe within the different compartments. The NMR method provides distinct pH values for the various organelles. The

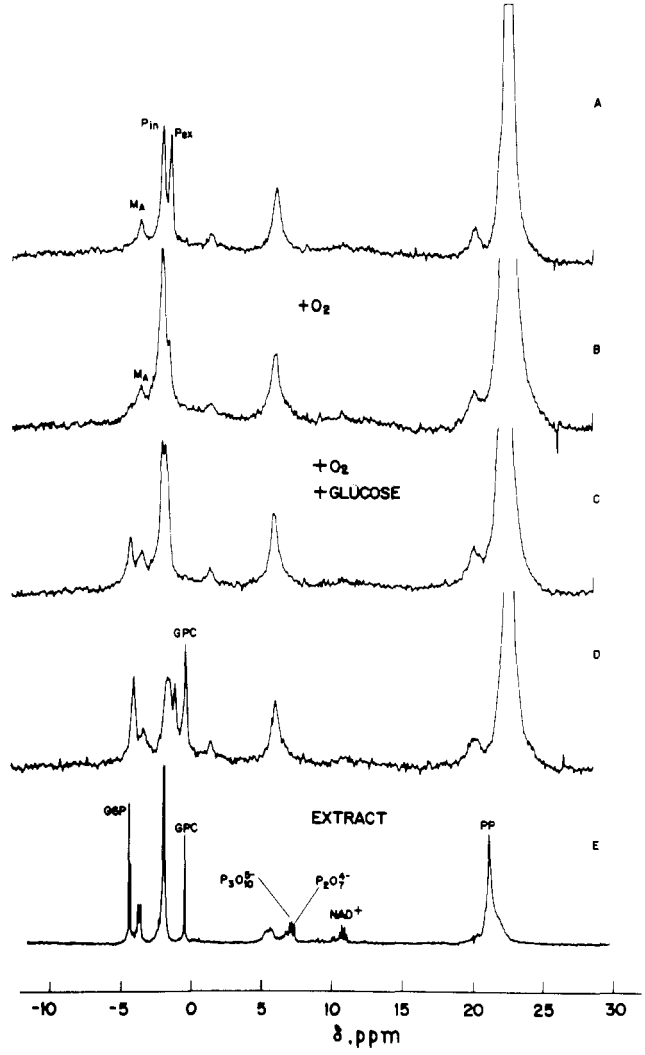

FIGURE 12: ^{31}P NMR spectra obtained for the *pgi* mutant. The strain was grown on YPFGal medium, and the cells were sedimented, washed with minimal medium, and then resuspended in phosphate buffer. Each whole-cell spectrum is the sum of 2000 scans. After 38 min, glucose was added to a final concentration of 50 mM. (A) Resting cells; (B) accumulations obtained between 21 and 32 min after starting O_2 bubbling; (C) accumulations obtained between 53 and 63 min; (D) accumulations obtained between 106 and 116 min (for calibration of the chemical shifts, 6 mM GPC was added to the suspension); and (E) extract prepared immediately after spectrum D was accumulated, with pH adjusted to 6.86.

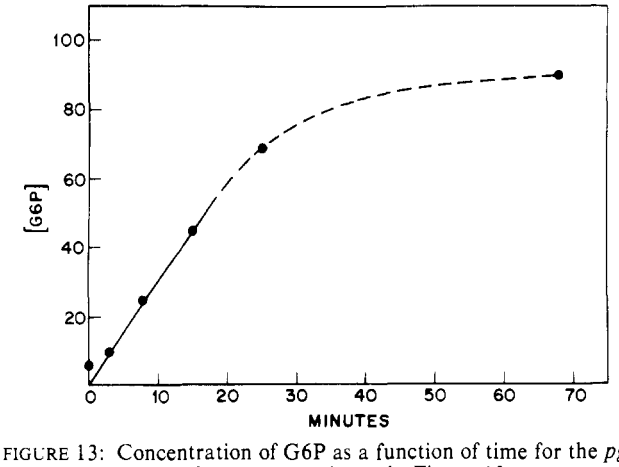

FIGURE 13: Concentration of G6P as a function of time for the *pgi* mutant determined from spectra shown in Figure 12.

observation of separate ^{31}P NMR signals for inorganic phosphate originating from the cytoplasm and organelles (liver

cell mitochondria) has recently been reported (Cohen et al., 1978).

The values of the intracellular pH reported in the present study seem to be higher than those reported previously based on other methods (Pena et al., 1972; Borst-Pauwels & Peters, 1977). In addition to some methodological difficulties in those reports, one should note that the pH values obtained were the average values of the cytoplasmic and organelle pH values.

It is interesting to note that the intracellular pH has a value of 7.3 in the presence of oxygen with an endogenous carbon source and only drops to ~7.2 when glucose is added, while the external pH drops to 3.6. The ability of the yeast cells to maintain such a pH difference indicates an active proton pump. The existence of an active proton pump in the plasma membrane of yeast cells is expected since the proton gradient is known to serve as the driving force in the transport of various metabolites such as amino acids and phosphate ions (Cockburn et al., 1975; Pena, 1976; Borst-Pauwels & Peters, 1977). The small decrease of the intracellular pH after the addition of glucose may be tentatively correlated with the decrease in the ATP level as indicated in Figure 2C. Oxygenation did not have any effect on the internal pH of the *pgi* mutant strain; neither did it result in the appearance of ATP peaks (Figure 12). This provides further support for the role of ATP in maintaining the pH gradient. The lack of ATP formation upon oxygenation in the *pgi* mutant strain is explained by the absence of functional mitochondria in this mutant.

It is seen in Figure 2 that after ~2 h under aerobic conditions, the external inorganic phosphate signal in wild-type cells is markedly diminished due to the transport of phosphate into the cells. Moreover, much of the inorganic phosphate is converted into polyphosphate (Figure 2D). This result agrees with the notion that polyphosphate serves in a storage capacity for inorganic phosphate. The possible role in energy storage through its high-energy phosphate bonds remains to be demonstrated.

From the NMR spectra of the yeast cell extracts it was possible to identify inner penultimate and terminal phosphates of the polyphosphate chains and oligomers (Figure 6B). Using the relative intensities of the peaks, we can estimate the average chain length of the polyphosphate molecules; a ratio of ~4:1 for the inner phosphates relative to the penultimate phosphates corresponds to an average length of ~12 phosphate residues. In the whole cells, the peak of the terminal phosphate groups of the polyphosphate is indistinguishable from those of the pyrophosphates, the terminal groups of tripolyphosphate, and ADP. However, the penultimate polyphosphate groups are resolved so that an estimate of the average polyphosphate chain length can be obtained from the intensity ratio of the penultimate to inner phosphate peaks. Thus, in wild-type cells (Figure 2) the ratio PP_5/PP_3 is ~5.5, corresponding to a chain length of ~13 phosphate residues. In Figure 10, there are extra peaks in the penultimate phosphate region which have yet to be assigned.

Upon addition of glucose to aerated cells, the internal inorganic phosphate concentration becomes reduced in all strains, except the *pgi* mutant. This reduction is by a factor of 2 or 3 in wild-type cells as seen in Figure 2 and confirmed in other experiments (data not shown). The reduction in intracellular inorganic phosphate is by almost 2 orders of magnitude for the *pfk* mutant (30–0.4 mM) (Figure 7C) and the *cif* mutant (Figure 10C). Low levels of P_i had been proposed by Racker (1965) as an explanation of the Pasteur effect, which is the slowing down of glucose metabolism by oxygen. The larger reduction in P_{in} in the *pfk* and *cif* mutants than in the wild-type strain is probably the result of the mutants accumulating hexose phosphates in order to overcome their metabolic blocks. However, the general reduction of P_{in} to concentrations of ~1 mM or lower does bring it into the concentration range in which it is likely to act as a positive allosteric effector of phosphofructokinase (Banuelos et al., 1977).

The specific assignment of peaks to metabolites is discussed under Results. An overview of these assignments, pointing out the qualitative agreement with expectations, is given here. The NMR spectra of resting cells always (Figures 2, 7, 9, and 12) showed a peak in the sugar phosphate region at the position of 3PGA. The introduction of glucose into the medium, with or without oxygen, resulted in peaks at the G6P position. For each strain except the *pgi* mutant, the G6P peaks, within minutes, evolved to a higher field position characteristic of F6P and FBP. In the *pgi* mutant, G6P is formed and remains by far the dominant peak in the sugar phosphate region (Figure 12D); this is to be expected for a mutant with negligible phosphoglucose isomerase activity. In general (except for the *pgi* mutant), the introduction of oxygen increased the ATP levels with corresponding reductions in the P_i peaks.

The stimulation by FBP of yeast pyruvate kinase activity is well-known (Haeckel et al., 1968; Hunsley & Suelter, 1969; Solomos, 1970), and a decrease in the concentration of FBP results in an increase in the amount of PEP (Solomos, 1970). In Figure 2B the wild-type strain K8 shows a PEP peak, upon oxygenation of the cells, which disappears (Figure 2C) after the introduction of glucose. It reappears ~1 h later under aerobic conditions when the glucose was probably exhausted and the levels of sugar phosphates were significantly reduced, as seen in Figure 2D. In the spectra for the *pfk* mutant, there was no detectable FBP (Figure 8B and text), but a PEP peak was observed (parts D and E of Figure 7). This is consistent with an absence of pyruvate kinase activity noted for this double mutant. In the spectra of the *cif* mutant (parts C and D of Figure 10), glucose is converted to FBP which builds up to very high levels and no PEP peak is observed.

Metabolism by the *pfk* mutant gives the most predictable results. Initially, 3PGA is observed in the resting cells. ATP is generated when endogenous glycolytic pathway intermediates are oxidized by respiration (parts A and B of Figure 7). The addition of glucose acts as a poison since all the ATP and P_{in} are used to generate sugar phosphates. The pattern does not change appreciably with time (parts C and D of Figure 7). The sugar phosphate region in the spectrum in Figure 8B shows no FBP, but G6P and F6P are detectable. Thus, the distribution of hexose phosphates is consistent with the mutant having a defect in its phosphofructokinase. There is a small amount of 6PGA (Figure 8B), which is the product of glucose-6-phosphate dehydrogenase, the first enzyme in the pentose shunt. There are three unassigned resonance peaks in the extract. It will be interesting to determine whether these peaks also represent intermediates in the pentose shunt. It seems unlikely that the appearance of 6PGA in the *pfk* mutant is a result of the accumulation of G6P in view of the fact that a similar accumulation of G6P in the *pgi* and *cif* mutants does not lead to the same effect. Thus, the activity of glucose-6-phosphate dehydrogenase, which is known to regulate the activity of the pentose phosphate pathway (Osmond & Rees, 1969), is likely to be higher in the *pfk* mutant strain. The ability of the *pfk* mutant strain to use hexoses as a carbon source could thus be explained by the increased activity of the pentose phosphate pathway. Recently, Oura (1976) has measured the glucose-6-phosphate dehydrogenase activity in wild-type yeast cells. Since he found the activity of this enzyme

to be relatively low and insensitive to levels of oxygen administered to the culture medium, he concluded that the pentose phosphate pathway has a negligible role as an energy-producing route but is important in providing NADPH for biosynthetic reactions. In the *pfk* mutant it seems that the pentose phosphate pathway could be acting as an important alternative energy-producing pathway. The upfield region of the *pfk* extract spectra (Figures 7 and 8B) is similar to that of the wild-type (Figures 2 and 8A), except that it shows much lower ATP and ADP intensities and smaller inner phosphate (Figure 7) and end-group polyphosphate signals (Figure 8B).

The *pgi* mutant shows the expected result, namely, that the addition of glucose generates a buildup of G6P and only very small amounts of other, still unidentified, metabolites. Since these cells have been grown fermentatively, their mitochondria are not functional. Thus, oxygenation does not stimulate any respiration. These cells appear energetically depressed, as seen from the absence of any ATP signal, a very small ADP signal, the diminished utilization of P_{in}, and the absence of several metabolites such as UDPG and other diphosphodiesters in the high-field regions of the spectrum (Figure 8D). The slow rate at which glucose is phosphorylated (Figure 13) is probably related to the lower level of ATP in the *pgi* mutant cells.

The observations for the *cif* mutant are most easily understood in terms of a futile cycle generated upon the addition of glucose to nonfermentatively grown cells. The *cif* mutation has been shown to prevent the inhibition of fructose bisphosphatase by glucose or fructose by enzymatic analysis. Since hexoses are the preferred carbon source for the growth of yeast cells, inhibition of this key gluconeogenic enzyme is necessary for the utilization of glucose and fructose. It is generally believed that in the wild-type strain when fructose bisphosphatase is inactivated, the rate of glycolysis is regulated by allosteric control of phosphofructokinase such that slower rates of reaction occur when the cell nears energy sufficiency. In the *cif* mutant in which fructose bisphosphatase is not inactivated, it is shown that the addition of glucose leads to lower ATP levels (Figures 8C and 10, Table IV); hence, phosphofructokinase is probably more active than in wild-type cells under similar conditions. Since the phosphofructokinase reaction proceeds with a large $\Delta G^{0'}$ (−3.4 kcal/mol), any available ATP is scavenged for the phosphorylation of F6P. This phosphorylation must also be stimulated by the increased concentration of F6P resulting from (a) the cleavage of FBP by fructose bisphosphatase into F6P and P_i and (b) the F6P produced from the increased influx of glucose by energy-depressed cells. This influx would also depress ATP levels. This sequence of events would explain the observations shown by the ^{31}P NMR spectra (Figures 8C and 10) and confirmed by enzymatic analysis of cell extracts (Table IV); namely, there is a dramatic rise in the level of FBP. Indeed, all glycolytic intermediates show elevated levels so that initially all glycolytic enzymes are active. Aldolase has normal activity in mutant cells exposed to glucose, and it is not inactivated by the accumulation of FBP (data not shown). Hence, it is proposed that the cell, deenergized as a consequence of the fructose bisphosphatase–phosphofructokinase futile cycle, increased the flux through phosphofructokinase so that a higher steady-state level of FBP is achieved. There are aspects of this proposed mechanism which remain to be tested, but it does explain all of the present observations.

The inactivation of fructose bisphosphatase is thought to involve a protease (Molano & Gancedo, 1974), but it has yet to be determined if the *cif* mutation affects the fructose bisphosphatase, the inactivating protease, or some component involved in the expression of the protease.

In conclusion, it has been shown how a ^{31}P NMR study of yeast glycolytic mutants complements the enzymatic analyses and strengthens the understanding of the metabolic disruptions brought about by glycolytic mutations.

References

Banuelos, M., Gancedo, C., & Gancedo, J. M. (1977) *J. Biol. Chem. 252*, 6394–6398.

Bergmeyer, H. U., Ed. (1974) *Methods of Enzymatic Analysis*, 2nd ed., Verlag Chemie, Weinheim/Bergstr., Germany.

Borst-Pauwels, G. W. F. H., & Peters, P. H. J. (1977) *Biochim. Biophys. Acta 466*, 488–495.

Burt, C. T., Glonek, T., & Barany, M. (1976) *J. Biol. Chem. 251*, 2584–2591.

Cockburn, M., Earnshaw, P., & Eddy, A. A. (1975) *Biochem. J. 146*, 705–712.

Cohen, S. M., Ogawa, S., Rottenberg, H., Glynn, P., Yamane, T., Brown, T. R., & Shulman, R. G. (1978) *Nature (London) 273*, 554–556.

Evans, F. F., & Kaplan, N. O. (1977) *Proc. Natl. Acad. Sci. U.S.A. 74*, 4969–4913.

Haeckel, R., Hess, B., Lauterborn, W., & Wuster, K.-H. (1968) *Hoppe*-Seyler's *Z. Physiol. Chem. 349*, 699–714.

Henderson, T. O., Costello, A. J. R., & Omachi, A. (1974) *Proc. Natl. Acad. Sci. U.S.A. 71*, 2487–2490.

Henry, S. A., Donahue, T. F., & Culbertson, M. R. (1975) *Mol. Gen. Genet. 143*, 5–11.

Hunsley, J. R., & Suelter, C. H. (1969) *J. Biol. Chem. 244*, 4819–4822.

Johnston, J. R., & Mortimer, R. K. (1959) *J. Bacteriol. 78*, 292.

Kudrna, R., & Edlin, G. (1975) *J. Bacteriol. 121*, 740–742.

Lam, K-B., & Marmur, J. (1977) *J. Bacteriol. 130*, 746–749.

Latzko, E., & Gibbs, M. (1974) *Methods of Enzymatic Analysis* (Bergmeyer, H. U., Ed.) 2nd ed., p 881, Verlag Chemie, Weinheim/Bergstr., Germany.

Lowry, O. H., Rosebrough, N. J., Farr, A. L., & Randall, R. J. (1951) *J. Biol. Chem. 193*, 265–275.

Maitra, P. K., & Lobo, Z. (1971) *J. Biol. Chem. 246*, 475–488.

Mitchell, P., & Moyle, J. (1969) *Eur. J. Biochem. 7*, 471–484.

Molano, J., & Gancedo, C. (1974) *Eur. J. Biochem. 44*, 213–217.

Moon, R. B., & Richards, J. H. (1973) *J. Biol. Chem. 248*, 7276–7278.

Navon, G., Ogawa, S., Shulman, R. G., & Yamane, T. (1977a) *Proc. Natl. Acad. Sci. U.S.A. 74*, 87–91.

Navon, G., Ogawa, S., Shulman, R. G., & Yamane, T. (1977b) *Proc. Natl. Acad. Sci. U.S.A. 74*, 888–891.

Navon, G., Navon, R., Shulman, R. G., & Yamane, T. (1978) *Proc. Natl. Acad. Sci. U.S.A. 75*, 891–895.

Needleman, R. B., & Tzagoloff, A. (1975) *Anal. Biochem. 64*, 545–549.

Osmond, C. B., & Rees, T. A. B. (1969) *Biochim. Biophys. Acta 184*, 35–42.

Oura, E. (1976) *Biotechnol. Bioeng. 18*, 415–420.

Pena, A. (1976) in *Mitochondria: Bioenergetics, Biogenesis and Membrane Structure* (Packer, L., & Gomez-Puyou, A., Eds.) pp 21–30, Academic Press, New York.

Pena, A., Cinco, G., Gomez-Puyou, A., & Tuena, M. (1972) *Arch. Biochem. Biophys. 153*, 413–425.

Perkins, D. D. (1949) *Genetics 34*, 607–626.

Racker, E. (1965) *Mechanisms in Bioenergetics*, p 253, Academic Press, New York.

Richards, O. C., & Rutter, W. J. (1961) *J. Biol. Chem. 236*, 3177–3184.
Rottenberg, H. (1975) *Biochim. Biophys. Acta*, 61–74.
Salhany, J. M., Yamane, T., Shulman, R. G., & Ogawa, S. (1975) *Proc. Natl. Acad. Sci. U.S.A. 72*, 4966–4970.
Serrano, R. (1977) *Eur. J. Biochem. 80*, 97–102.
Solomos, T. (1970) *Biochem. Biophys. Res. Commun. 40*, 1076–1083.
Ugurbil, K., Rottenberg, H., Glynn, P., & Shulman, R. G. (1978) *Proc. Natl. Acad. Sci. U.S.A. 75*, 2244–2248.
van de Poll, K. W., & Schamhart, D. H. J. (1977) *Mol. Gen. Genet. 154*, 61–66.

Deoxyribonucleic Acid Repair Synthesis in Permeable Human Fibroblasts Exposed to Ultraviolet Radiation and *N*-Acetoxy-2-(acetylamino)fluorene†

John D. Roberts‡ and Michael W. Lieberman*

ABSTRACT: We have studied deoxyribonucleic acid (DNA) repair synthesis in permeable, confluent normal and repair-deficient human fibroblasts using [^{3}H]dCTP, BrdUTP, dATP, and dGTP as substrates. In this system repair synthesis occurred as judged by the following criteria: (1) labeled nucleotides were incorporated into parental DNA (ρ = 1.73 g/cm^3 in alkaline CsCl); (2) incorporation into parental DNA was negligible in the absence of damage and increased 10–20-fold in normal cells following exposure to ultraviolet radiation (UV) or the direct-acting chemical carcinogen *N*-acetoxy-2-(acetylamino)fluorene; and (3) damage-dependent DNA synthesis was absent in preparations made from excision repair-deficient human diploid fibroblasts (xeroderma pigmentosum cells, complementation group A). The reaction was linear for 10 min and continued for at least 1 h. Repair synthesis was stimulated at least fivefold by the addition of 5 mM ATP. It was strongly Mg^{2+} dependent, inhibited by NaCl, and only partially dependent upon the addition of exogenous dNTPs. The pH optimum in Tris-HCl buffer was 7.6. Following damage (UV), labeled deoxycytidine and dCMP were incorporated into parental DNA but at reduced levels (38 and 88%, respectively) compared to dCTP. The addition of β-NAD$^+$ (the naturally occurring isomer) or α-NAD$^+$ (a competitive inhibitor) had little effect on repair synthesis in this system. By saturating the system with dNTPs and using published estimates of patch size, we calculated that in this system a normal cell can put in a minimum of 100–900 repair patches/min.

Although recent studies have greatly increased our understanding of DNA repair processes (Hanawalt et al., 1978, 1979; Nichols & Murphy, 1977; Setlow, 1978), the detailed molecular events of eucaryotic excision repair are still unclear. Investigations of the role of chromatin structure in repair (Mortelmans et al., 1976; Bodell, 1977; Cleaver, 1977; Smerdon et al., 1978; Smerdon & Lieberman, 1978a; Tlsty & Lieberman, 1978) have emphasized the importance of studying molecular mechanisms in systems which closely approximate conditions in the living cell. Studies of DNA replicative synthesis in permeable mammalian cells and nuclei (Seki et al., 1975; Krokan et al., 1975; Tseng & Goulian, 1975; Berger & Johnson, 1976) have prompted us, as well as others (Ciarrocchi & Linn, 1978; Smith & Hanawalt, 1978), to use this approach to study DNA repair. In this paper, we report our initial observations on DNA repair synthesis in permeable normal and xeroderma pigmentosum fibroblasts (XP) treated with ultraviolet radiation and the chemical carcinogen *N*-acetoxy-2-(acetylamino)fluorene (NA-AAF)[1]. We have examined in detail the criteria for repair synthesis, cofactor requirements, and the rate of repair synthesis in this system.

Materials and Methods

Cell Culture and Preparation of Prelabeled Cells. Human diploid fibroblasts (IMR-90; Institute for Medical Research, Camden, NJ; Nichols et al., 1977) and xeroderma pigmentosum fibroblasts (XP12BE, complementation group A; American Type Culture Collection, Rockville, MD) were used between passages 15 and 24. Fibroblasts were grown to confluence as previously described (Amacher et al., 1977). To label parental DNA, we split cells (1:2 or 1:3) and exposed them to 2.5 nCi/mL [^{14}C]thymidine (50–60 mCi/mmol, New England Nuclear or Amersham) during growth. The medium was changed, and the cells were allowed to come to confluence. Conditions were adjusted so that the specific activity of the DNA was in the range of 100–200 cpm/μg. Cells were used within 10 days after reaching confluence.

UV Irradiation and Chemical Damage. Confluent cells, prelabeled with [^{14}C]thymidine, were treated with 10^{-4} M BrdUrd (Sigma) (final concentration) for ~3 h prior to damage. Incidental exposure to room lighting was minimized. To damage the cells with UV, we removed the medium and washed the cells once with ice-cold phosphate-buffered saline (PBS) (2.7 mM NaH_2PO_4, 13.1 mM Na_2HPO_4, 135 mM

† From the Department of Pathology, Washington University School of Medicine, St. Louis, Missouri 63110. *Received April 3, 1979.* This study was supported by National Institutes of Health Grant CA 20513 and by the following companies: Brown and Williamson Tobacco Corp.; Larus and Brother Co., Inc.; Phillip Morris, Inc.; Lorillard, a Division of Loews Theatres, Inc.; Liggett & Myers, Inc.; R. H. Reynolds Tobacco Co.; United States Tobacco Co.; and Tobacco Associates, Inc. Media, cells, and electron microscopy were provided by the Washington University Cancer Center (supported by National Institutes of Health Grant 20513).
‡ Supported by National Institutes of Health Predoctoral Fellowship ES 07066.

[1] Abbreviations used: NA-AAF, *N*-acetoxy-2-(acetylamino)fluorene; Me_2SO, dimethyl sulfoxide; XP, xeroderma pigmentosum; dNTPs, the four deoxyribonucleoside 5′-triphosphates; PBS, phosphate-buffered saline.

0006-2960/79/0418-4499$01.00/0